EFFECT OF GAS COMPOSITION AND TEMPERATURE ON REDUCTION CHARACTERISTIC IN RED MUD–COAL COMPOSITE PELLETS

Yi MAN*[*1]; Jun-xiao FENG[2]; Zhan-min YANG[1] ; Zeng-lu SONG[1] ; Chao YANG[1]

[*1] Nanjing Institute of Industry Technology, Jiangsu 210000, China

[2] School of Energy and Environmental Engineering, University of Science and Technology Beijing, Beijing 100083, China

[*] Corresponding author; E-mail: bestmanyi@sina.com

Abstract: The disposal of red mud, which is the by-product obtained from alumina production, has brought about environmental pollution because of its caustic nature as well its metal and alkaline contents. Red mud–coal composite pellets were directly reduced to deal with red mud. The influences of reduction temperature and gas composition on the reaction were studied. Experiment results indicated that the optimum reaction parameters were a temperature of 1100 °C and an H_2 atmosphere. Reduction degrees in H_2 and CO atmospheres were significantly higher than those in N_2 atmosphere. Reduction did not strictly follow the $Fe_2O_3 \rightarrow Fe_3O_4 \rightarrow FeO \rightarrow Fe$ sequence in N_2 atmosphere, and this phenomenon did not occur in H_2 atmosphere. This gas–solid combination reduction process is appropriate for recovering Fe from Bayer red mud. Meanwhile, the microstructure and phase transformation of the reduction process were investigated via scanning electron microscopy and X-ray diffraction.

Key words: Reduction characteristics; Red mud; Direct reduction; Bayer process; Kinetics analysis

1. Introduction

With the development of economic, Alumina has been an important raw material. With the domestic and overseas increasing demand for alumina, the alumina industry developed rapidly over the past 10 years [1–2]. Red mud, the main by-product of alumina production, is mainly composed of iron (Fe), aluminum (Al), titanium, silicon, calcium oxide, and hydroxide [3–5]. Red mud is a kind of highly alkaline waste product. The pH is typically between 10.0 and 12.5. It is regarded as a hazardous substance that requires careful handling because of its high alkaline content [6–9]. Using red mud has both environmental and economic significance [10–12]. During the last few decades, red mud has been applied for various purpose, such as adsorbent for water and gas treatment [13–19], catalyst for certain reactions [20–25], and material for building construction and ceramics [26–28]. At present, red mud is also used in metallurgy. Recovering metals are typically recovered from Bayer red mud through direct reduction. In addition, residues left after the separation processes are reused as building materials. Liu [29] conducted an simulative and experimental research on the phase changes of Bayer red mud roasting system and alumina, sodium, and Fe recovery. Li [30] investigated the recovery behavior of ferric oxide (Fe_2O_3) and alumina from Bayer red mud through reduction sintering. Zhu [31] studied the synthesis process of sodium carbonate addition–roasting reduction–magnetic separation to treat Fe-

rich red mud and recover Fe from it. Liu [32] proposed a process to recycle Fe from red mud through magnetic separation, in which Fe_2O_3 in red mud is transformed into magnetite (Fe_3O_4) through anaerobic coroasting with pyrite. Qiu [33] determined the effect of coal type on direct reduction of red mud with high Fe content. Samouhos [34] developed a microwave reductive roasting technique for red mud by using lignite to recover metallic Fe. Yang [35] presented a coal-based direct reduction technique used for recovery and reuse of Fe in vanadium tailings. Process parameters, such as additive use, tailings/additives/reductant proportion, reduction time, reduction temperature, particle size were experimentally studied. The direct reduction method is an effective means to develop a wide range of applications for red mud. Therefore, studying reduction characteristics is necessary. In this study, the influences of reduction parametersgas, especially the gas composition and temperature on the reduction process in red mud–coal composite pellets were investigated.

2. Materials and experiments

2.1. Materials

The Bayer process Red mud used in the research was obtained from Shandong, China. The chemical constituents of red mud was mainly 47.6% TFe, 1.20% FeO, 10.4% SiO_2, 1.44 CaO, 9.42% Al_2O_3, 0.42% MgO, 1.73% Na_2O, 0.24% K_2O, 1.31% TiO_2, 0.026% S, and 0.023% P. The particle size was in the range of 75 ~ 150 μm. The crystalline phase was investigated via X-ray diffraction by the application of Cu-Kα radiation operated at 40 kV and 150 mA. Several mineral phases were observed, such as anatase, cancrinite, hematite, quartz, limonite and diaspore, as shown in Fig. 1. The reducing agent selected for this analysis was bituminous coal, which was obtained from Shanxi, China. The main composition of bituminous coal was 74.48% fixed carbon (C), 12.51% volatile matter, and 13.01% ash. The mean size was 109 μm. The coal was evaporated in nitrogen for 2 h at 600°C before mixed.

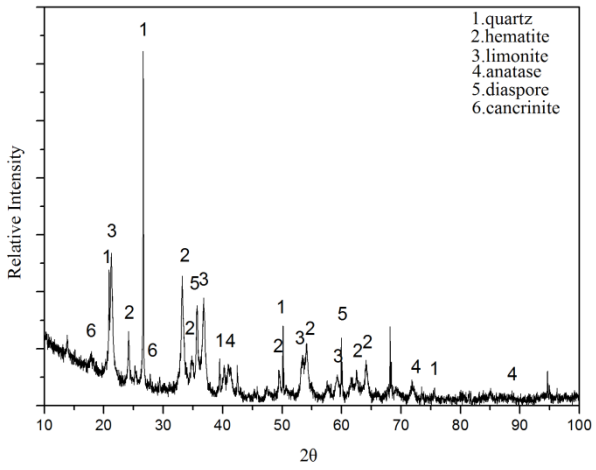

Fig. 1. XRD pattern of red mud

2.2. Experiments

Throughout the study, the mixture of oxygen (O) (O_{TFe}) and fixed C (C_{Fix}) in red mud particles were used. The mole ratio was 1:1 in nitrogen and 0.5:1 in the reducing atmosphere. Pellets with a diameter of 15 mm were made from red mud–coal and 1.5% bentonite binder mixture in a disc

pelletizer with the following parameters: rim height = 300 mm, diameter = 1000 mm, rotation frequency = 28 rpm and inclination angle = 45°. The pellets were stoved in an oven at 250°C for 3 h. After cooling, the pellets were stored in a desiccator prior for use. The experiments were conducted at temperatures from 700 °C to 1100 °C.

Experimental research introduced in this study was performed in the thermogravimetric analyzer apparatus. This apparatus comprised an electronic balance, a temperature controller, an electric furnace, a gas distributor disk, and a quartz glass tube reactor. Three groups of experiments (N_2, H_2 and CO) were carried out to study the effects of different gas compositions on reducing Fe in red mud. The oven was heated to the required temperature. Afterwards, the experimental pellets were put into the heating zone. Gas flow was maintained at 1 L/min. The weights of the experimental pellets were recorded every one minute. After the experiment, the experimental pellets were taken out of the oven and cooled to indoor temperature in N_2 atmosphere.

The reduction degree of production was calculated according to Eq. (1) as follows [36]:

$$\alpha = \frac{(W_0 - W_t)}{oxygen(mass) + carbon(mass)} \times 100 \qquad (1)$$

where α is reduction degree of production (%), W_0 is initial mass of the samples after removing moisture, and W_t is quality of the samples after each time t. Oxygen(mass) was estimated for the total mass of O appeared in forms of FeO, Fe_2O_3, and Fe_3O_4.

3. **Results and discussion**

3.1. Effects of gas composition on reduction

Effects of gas composition were studied by monitoring the mass changes in the isothermal reduction. The reduction degree α from 700 °C to 1100 °C are shown in Figs. 2 to 5.

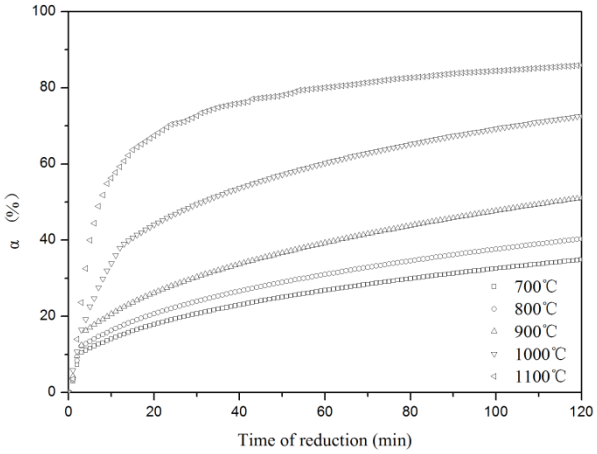

Fig. 2. Fe recovery in N_2 atmosphere

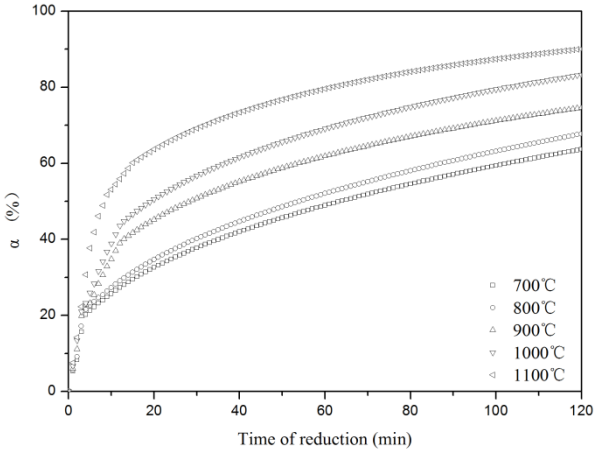

Fig. 3. Fe recovery in CO atmosphere

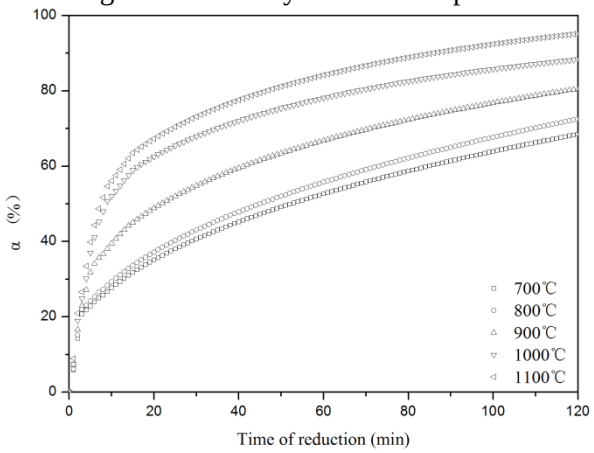

Fig. 4. Fe recovery in H_2 atmosphere

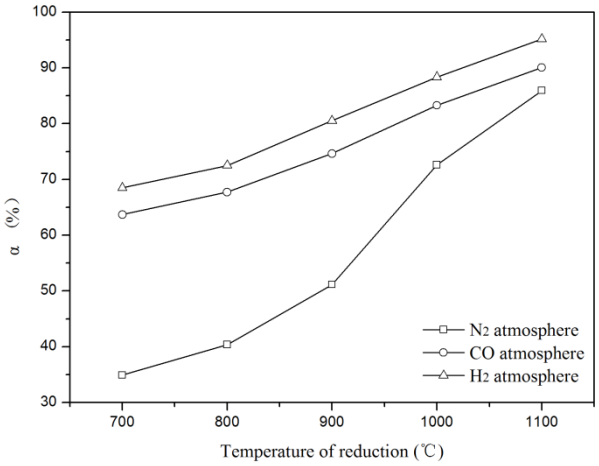

Fig. 5. Fe recovery in different gas composition for 120 minute

These figures show that as the temperature raised from 700 °C to 1100 °C, the reduction degree for all the samples increased in different atmospheres. When the three samples were heated under the same conditions to recover Fe, the reduction degrees in CO and H_2 atmospheres were 63.69% and 68.48%, respectively, at 700 °C, which were significantly higher than that in N_2 atmosphere (34.89%). The same conclusion can be drawn in other temperatures. Thus, the reduction degrees in H_2 and CO atmospheres are significantly higher than that in the N_2 atmosphere. The reduction degree exhibits a maximum value in H_2 atmosphere at the same temperature.

3.2. Comparison in Arrhenius activation energy

The kinetics equation can be employed to analyze the kinetic data and to definit the reduction mechanisms of red mud–coal composite pellets in different atmospheric conditions. The 3D diffusion reaction model developed by Jender and Anorg was selected for this study. The model can be expressed by the following equation:

$$\left[1-(1-\alpha)^{1/3}\right]^2 = kt\,, \qquad (2)$$

where t is time (s), and k is rate constant (s^{-1}). Apparent activation energy values were calculated according to the Arrhenius equation as follow:

$$\ln k = \ln A - \frac{E}{RT}\,, \qquad (3)$$

The plots of ln (k) versus 1/T are shown in Fig. 6. Slopes were applied to calculate the activation energy.

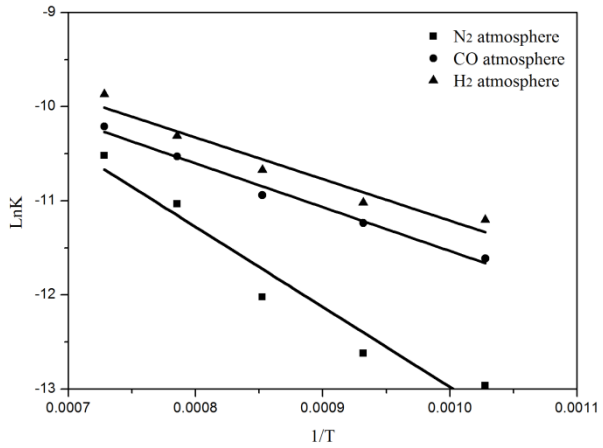

Fig. 6. Arrhenius plots for reducing red mud–coal composite pellets

A value of 70.72 kJ/mol was obtained by reducing red mud–coal composite pellets in N_2 atmosphere. The values of 38.65 kJ/mol and 36.73 kJ/mol were used to calculate the gas compositions of CO and H_2, respectively. The results show that the activation energy of reduction decreased significantly in a reducing atmosphere.

3.3. XRD characterization of the samples

After comparing the aforementioned reduction conditions, the heated residues in N_2 and H_2 atmospheres were selected for X-ray diffraction analysis. The X-ray diffraction patterns of the residues are presented in Fig. 7. The peaks of hematite and some minor constituents, such as cancrinite, anatase and diaspore disappeared in the heated residues. Phase compositions of the two groups of samples are different. As shown in Fig. 7(a), the residues were Fe_3O_4 and SiO_2 at 700 °C, whereas Fe_3O_4 peaks were reduced at over 800 °C. The presence of FeO at 900 °C confirmed that the reduction of Fe_3O_4, which formed the FeO, was initiated at below 900 °C. The metallic Fe phase appeared when temperature increased to 1000 °C. However, Fe_3O_4 still remained. At 1100 °C, the Fe_3O_4 phase in the heated residues completely disappeared. Metallic Fe dominated the sample. However, small amounts of FeO still remained. In Fig. 7(b), the XRD patterns of five reduced samples at 700, 800, 900, 1000, and 1100 °C are presented. No noticeable difference was observed in the XRD patterns. The main component in all samples was metallic Fe.

The reduction rate in H_2 atmosphere was significantly faster than in N_2 atmosphere.

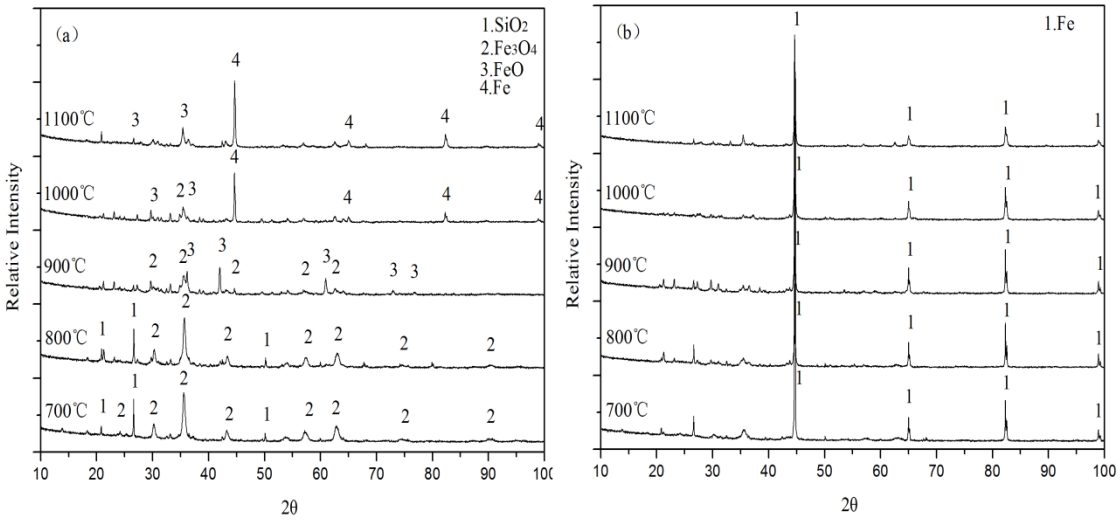

Fig. 7. X-ray diffraction patterns of heated residues: (a) Nitrogen, (b) Hydrogen

3.4. Scanning electron microscopy analysis

The scanning electron microscopy (SEM) images of the heated residues and the raw material are shown in Fig. 8. The unreacted red mud particles agglomerated with one another irregularly, as shown in Fig. 8(a). The principal phases in red mud revealled no any significant change at 700 °C in Fig. 8(b). As the gas generated during reaction volatilized, a few small pores were observed within the particles at 900 °C in Fig. 8(c). In Fig. 8(d), the residues were light sintered and exhibited a porous structure and a granularity increscent appearance at 1000 °C. At 1100 °C, the heated residues exhibited a developed porous system and several bright areas appeared, as shown in Fig. 8(e), thus showing that the reduction reached quite high level. The SEM images of the heated samples under optimized H_2 atmosphere conditions are shown Figs. 8(f) to 8(h). As shown in the figures, the heated samples displayed a developed porous structure even at 700 °C. The SEM images of the residues heated in H_2 atmosphere exhibited a looser surface and porous system compared with the images of the residues heated in N_2 atmosphere.

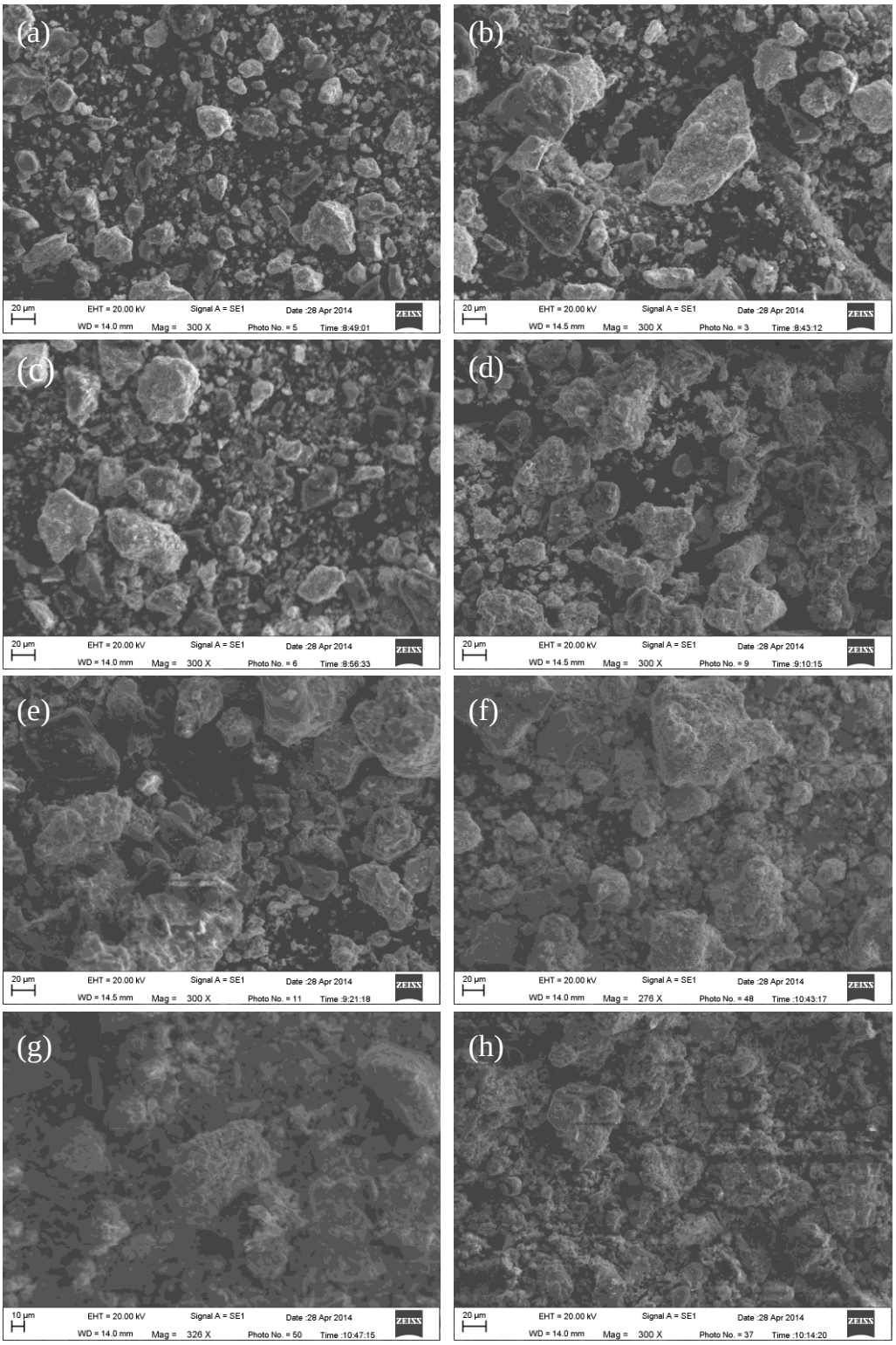

Fig. 8. SEM analysis of sample pellets: (a) 20 °C Nitrogen, (b) 700 °C Nitrogen, (c) 900 °C Nitrogen, (d) 1000 °C Nitrogen, (e) 1100 °C Nitrogen, (f) 700 °C Hydrogen, (f) 900 °C Hydrogen, and (g) 1100 °C Hydrogen.

4. **Conclusions**

Red mud, which is the abundant waste product in aluminum industry, can be used as a raw material to reduce Fe directly. According to the results of this experiment, the conclusions can be drawn as follows.

(1) XRD analyses and thermogravimetric experiments show that the temperature of 1100 ℃ and an H_2 atmosphere are optimum parameters for reducing red mud–coal composite pellets under the experiment conditions.

(2) In N_2 atmosphere, reduction does not strictly follow the $Fe_2O_3 \rightarrow Fe_3O_4 \rightarrow FeO \rightarrow Fe$. Fe_3O_4 sequence. Fe and FeO can coexist in some parts of the pellet during the reduction process. However, this phenomenon does not occur in reducing H_2 atmosphere.

(3) Fe_2O_3 reduction, which forms Fe_3O_4, is completed at below 700 ℃ in N_2 atmosphere. The presence of FeO confirms that the reduction of Fe_3O_4, which forms FeO, is initiated at below 900 ℃. The Fe_3O_4 phase disappears at 1100 ℃ and metallic Fe dominates the sample, thus showing that the product has reached quite high reduction degree. In H_2 atmosphere, FeO reduction, which forms Fe, occurs at below 700 ℃.

(4) Fe from Bayer red mud is reduced in three different gas compositions. Reduction temperature and gas composition are the two main factors that affect Fe reduction. Through the three groups used in the experiments, the results obtained from the reducing atmosphere for red mud–coal composite pellets are more advantageous than those obtained from red mud in a previous study. This gas–solid combination reduction process exhibits a reasonable reduction phase and high reduction degree.

Acknowledgment

Project supported by the University Natural Science Foundation of Jiangsu Province, China (Grant No.18KJD450002).

References

[1] Liu,W.C., *et al*., Application of Bayer red mud for iron recovery and building material production from alumosilicate residues, Journal of Hazardous Materials, 161(2009), 1, pp. 474-478

[2] Cao,S.T., *et al*., The phase transition in Bayer red mud from China in high caustic sodium aluminate solutions, Hydrometallurgy, 140(2013), pp. 111-119

[3] Qu,Y., *et al*., Bioleaching of heavy metals from red mud using Aspergillus niger,Hydrometallurgy, 136(2013), pp. 71-77

[4] Álvarezj,J., *et al*., A new method for enhancing the performance of red mud as a hydrogenation catalyst, Applied Catalysis A: General, 180(1999), 1-2, pp. 399-409

[5] Cao,J.L., *et al*., Mesoporous modified-red-mud supported Ni catalysts for ammonia decomposition to hydrogen, International journal of hydrogen energy, 39(2014), 11, pp. 5747-5755

[6] Liu,Y., *et al*., Characterization of red mud derived from a combined Bayer Process and bauxite calcination method, Journal of Hazardous Materials, 146(2007), 1-2, pp. 255-261

[7] Liu,X.M., *et al*., Structural investigation relating to the cementitious activity of bauxite residue-Red mud, Cement and Concrete Research, 41(2011), 8, pp. 847-853

[8] Borges,A.J.P., *et al*., Cleaner red mud residue production at an alumina plant by applying experimental design techniques in the filtration stage, Journal of Cleaner Production, 19(2011), 15, pp. 1763-1769.

[9] Hajjaji,W., *et al*., Composition and technological properties of geopolymers based on metakaolin and red mud, Materials and Design, 52(2013) , pp. 648–654

[10] Maddocks,G., *et al*., Effect of Bauxsol TM and biosolids on soil conditions of acid-generating mine spoil for plant growth, Environmental Pollution, 127(2004), 2 , pp. 157-167

[11] Sglavo,V.M., *et al*., Bauxite 'red mud' in the ceramic industry. Part 1: thermal behavior, Journal of the European Ceramic Society, 20(2000), 3, pp. 235-244

[12] Renforth,P., *et al*., Contaminant mobility and carbon sequestration downstream of the Ajka (Hungary) red mud spill: The effects of gypsum dosing, Science of the Total Environment, 421-422(2012), pp. 253-259

[13] Deihimi,N., *et al*., Characterization studies of red mud modification processes as adsorbent for enhancing ferricyanide removal, Journal of Environmental Management, 206(2018), pp. 266-275

[14] Li,H.N., *et al*., Degradation of bezafibrate in wastewater by catalytic ozonation with cobalt doped red mud: Efficiency, intermediates and toxicity, Applied Catalysis B: Environmental, 152-153(2014), pp. 342-351

[15] Justyna,P.O., *et al*., Assessing the role of bed sediments in the persistence of red mud pollution in a shallow lake (Kinghorn Loch, UK), Water Research, 123(2017), pp. 569-577

[16] Luo,L., *et al*., New insights into the sorption mechanism of cadmium on red mud, Environmental Pollution, 159(2011), 5, pp. 1108-1113

[17] Lv,G.C., *et al*., Preparation and characterization of red mud sintered porous materials for water defluoridation, Applied Clay Science, 74(2013), pp. 95-101

[18] Sahu,R.C., *et al*., Removal of hydrogen sulfide using red mud at ambient conditions, Fuel Processing Technology, 92(2011), 8, pp. 1587-1592

[19] Zhang,L.Y., *et al*., Removal of malachite green and crystal violet cationic dyes from aqueous solution using activated sintering process red mud, Applied Clay Science, 93-94(2014), pp. 85-93

[20] Olivera,A.A.S., *et al*., Biphasic oxidation reactions promoted by amphiphilic catalysts based on red mud residue, Applied Catalysis B: Environmental, 144(2014), pp. 144-151

[21] Teixeira,I.F., *et al*., Carbon deposition and oxidation using the waste red mud: A route to store, transport and use offshore gas lost in petroleum exploration, Fuel, 124(2014), pp. 7-13

[22] Sushil,S., *et al*., Catalytic applications of red mud, an aluminium industry waste: A review, Applied Catalysis B: Environmental, 81(2008), 1-2, pp. 64-77

[23] Liang,W., *et al*., Effect of strong acids on red mud structural and fluoride adsorption properties, Journal of Colloid and Interface Science, 423(2014), pp. 158-165

[24] Karimi,E., *et al*., Ketonization and deoxygenation of alkanoic acids and conversion of levulinic acid to hydrocarbons using a Red Mud bauxite mining waste as the catalyst, Catalysis Today, 190(2012), 1, pp. 73-88

[25] Song,J., *et al*., Red mud enhanced hydrogen production from pyrolysis of deep-dewatered sludge cakes conditioned with Fenton's reagent and red mud, International journal of hydrogen energy, 41(2016), 38, pp. 16762-16771

[26] Yao,Y., *et al*., Characterization on a cementitious material composed of red mud and coal industry byproducts, Construction and Building Materials, 47(2013), pp. 496-501

[27] David D.A., *et al*., Awaso bauxite red mud-cement based composites: Characterisation for pavement applications, Case Studies in Construction Materials, 7(2017), pp. 45-55

[28] Zhang,N., *et al*., Pozzolanic behaviour of compound-activated red mud-coal gangue mixture, Cement and Concrete Research, 41(2011), 3, pp. 270-278

[29] Liu,W.C., *et al*., Experimental and simulative study on phase transformation in Bayer red mud soda-lime roasting system and recovery of Al, Na and Fe, Minerals Engineering, 39(2012), pp. 213-218

[30] Li,X.B., *et al*., Recovery of alumina and ferric oxide from Bayer red mud rich in iron by reduction sintering, Transactions of Nonferrous Metals Society of China, 19(2009), 5, pp. 1342-1347

[31] Zhu,D.Q., *et al*., Recovery of Iron From High-Iron Red Mud by Reduction Roasting With Adding Sodium Salt, Journal of Iron and Steel Research, International, 19(2012), 8, pp. 1-5

[32] Liu,Y.Y., *et al*., Recycling of iron from red mud by magnetic separation after co-roasting with pyrite, Thermochimica Acta, 588(2014), pp. 11–15

[33] Qiu,G.Z., *et al*., Influence Of Coal Sort on The Direct Reduction of High-Iron-Content Red Mud, J Cent South University Technol, 2(1995), pp. 27-31

[34] Samouhos,M., *et al*., Greek “red mud” residue: A study of microwave reductive roasting followed by magnetic separation for a metallic iron recovery process, Journal of Hazardous Materials, 254-255(2013), pp. 193-205

[35] Yang,H.F., *et al*., Recovery of iron from vanadium tailings with coal-based direct reduction followed by magnetic separation, Journal of Hazardous Materials, 185(2011), 2-3, pp. 1405-1411

[36] El-Hussiny,N.A., *et al*., A Self-Reduced Intermediate Product from Iron and Steel Plants Waste Materials Using a Briquetting Process, Powder Technology, 205(2011), 1-3, pp. 217-223